

·基础研究·

基于PERK/eIF2 α /ATF4/CHOP通路探讨健骨颗粒对UMR-106细胞内质网应激凋亡的影响

陈赛楠^{1,2,3}, 周芬^{1,2,4}, 黄云梅^{1,2}, 林燕萍^{1,2*}

1 福建中医药大学中西医结合研究院, 福建 福州 350122;
2 福建省中西医结合老年性疾病重点实验室, 福建 福州 350122;
3 福建省中医药科学院骨质疏松证候基因组学重点研究室, 福建 福州 350003;
4 福建中医药大学杂志社, 福建 福州 350122
* 通信作者: 林燕萍, E-mail: linyanping1966@163.com

收稿日期: 2023-07-08; 接受日期: 2023-11-15

基金项目: 国家自然科学基金项目(81574003); 福建省财政专项资助项目(X2019002-财政专项)

DOI: 10.3724/SP.J.1329.2024.01006

开放科学(资源服务)标识码(OSID):



摘要 **目的** 探讨健骨颗粒含药血清对UMR-106成骨样细胞内质网应激ERS凋亡的影响和作用机制。**方法** 选用UMR-106成骨样细胞, 采用0、0.01、0.02、0.03、0.04、0.05 $\mu\text{mol/L}$ 不同浓度的GSK2606414(PERK抑制剂)对细胞进行干预, 采用CCK8法筛选GSK2606414最佳干预浓度。将生长状态较好的UMR-106细胞随机分为阴性对照组(NC组)、模型组(H_2O_2 组)、健骨颗粒组(H_2O_2 +JG组)和阳性对照组(H_2O_2 +GSK2606414组)4组。NC组和 H_2O_2 组采用10%生理盐水血清干预12 h, H_2O_2 +JG组采用10%健骨颗粒含药血清干预12 h, H_2O_2 +GSK2606414组采用0.03 $\mu\text{mol/L}$ 的GSK2606414和10%生理盐水血清干预12 h, 除NC组外, 其余各组在不更换新培养基的情况下, 再分别加入10 $\mu\text{mol/L}$ H_2O_2 干预12 h。采用激光共聚焦显微镜观察细胞内NC组和 H_2O_2 组GRP78和Caspase-12荧光表达情况, DCFH-DA检测活性氧(ROS)含量, 激光共聚焦显微镜观察细胞内钙离子实时动态变化判断ROS/ERS模型是否成立。再采用Annexin V-FITC/PI检测4组细胞晚期凋亡率, qPCR和Western blot检测4组ERS相关标志指标GRP78、PERK、eIF2 α 、ATF4和CHOP mRNA转录水平和蛋白相对表达量。**结果** 与0 $\mu\text{mol/L}$ 组比较, 0.03 $\mu\text{mol/L}$ 的GSK2606414是干预UMR-106细胞12 h后对细胞活力没有影响的最大浓度, 故使用该浓度作为后续 H_2O_2 +GSK2606414组的实验干预条件。与NC组相比, H_2O_2 组ROS含量显著增高($P<0.01$), GRP78和Caspase-12的蛋白荧光表达量明显增加, 细胞内钙离子流动速度加快并持续增高, 表明 H_2O_2 诱导UMR-106细胞ROS/ERS模型的成功建立。与NC组相比, H_2O_2 组凋亡率显著增高($P<0.05$), GRP78、PERK、eIF2 α 、ATF4、CHOP mRNA转录水平和蛋白相对表达量均显著增高($P<0.01$)。与 H_2O_2 组相比, H_2O_2 +JG组和 H_2O_2 +GSK2606414组ROS含量显著降低($P<0.01$), 凋亡率显著降低($P<0.05$), GRP78、PERK、eIF2 α 、ATF4、CHOP mRNA转录水平($P<0.05$)和蛋白相对表达量($P<0.01$)均显著降低。**结论** 健骨颗粒可通过PERK/eIF2 α /ATF4/CHOP信号通路缓解内质网过度应激, 降低成骨细胞凋亡率, 发挥防治绝经后骨质疏松症的作用。

关键词 绝经后骨质疏松症; 内质网应激; 健骨颗粒; PERK/eIF2 α /ATF4/CHOP信号通路; 成骨细胞凋亡

绝经后骨质疏松症(postmenopausal osteoporosis, PMOP)是雌激素水平急剧降低引发骨量下降和

骨微结构破坏, 致使骨强度减弱和脆性骨折发病率增加的全身性代谢性疾病, 属于高转换型原发性骨

引用格式: 陈赛楠, 周芬, 黄云梅, 等. 基于PERK/eIF2 α /ATF4/CHOP通路探讨健骨颗粒对UMR-106细胞内质网应激凋亡的影响[J]. 康复学报, 2024, 34(1): 34-43.
CHEN S N, ZHOU F, HUANG Y M, et al. Jiangu granules regulates endoplasmic reticulum stress-induced apoptosis in UMR-106 cells by modulating the PERK/eIF2 α /ATF4/CHOP pathway [J]. Rehabil Med, 2024, 34(1): 34-43.
DOI: 10.3724/SP.J.1329.2024.01006

质疏松症^[1]。破骨细胞介导骨吸收和成骨细胞介导骨形成是维持骨稳态的重要因素,雌激素在其中发挥至关重要的作用,PMOP发生时骨吸收量和骨形成量均增强,但是骨吸收量大于骨形成量。雌激素还是一种抗氧化剂^[2],雌激素水平降低和衰老等因素会导致机体活性氧(reactive oxygen species, ROS)过度堆积^[3],氧化还原平衡被打破,进一步诱发内质网应激(endoplasmic reticulum stress, ERS),近十年来许多研究显示ERS与PMOP的发生和发展关系密切^[4-5]。

内质网的蛋白质合成、折叠和修饰等功能的正常发挥是细胞存活的必要条件,氧化还原状态的改变和钙离子流动异常等引起内质网中未折叠蛋白或错误折叠蛋白堆积,从而触发未折叠蛋白反应(unfolded protein response, UPR),轻度的UPR可维持细胞稳态,然而持续、过强的UPR引起细胞凋亡;因成骨细胞分泌大量的细胞外基质蛋白,特别容易受到ERS引起的功能障碍影响,阻碍其增殖分化甚至凋亡,从而导致PMOP的发生和发展。PERK/eIF2 α /ATF4/CHOP通路是ERS的最主要的信号通路之一,同样在骨代谢调控中起关键作用^[6],为调控ERS相关疾病如PMOP提供新思路。

健骨颗粒是治疗PMOP的经验方,临床效果显著,课题组前期研究显示健骨颗粒可有效清除机体内多余ROS,并且对肿瘤坏死因子- α (tumor necrosis factor- α , TNF- α)诱导的成骨细胞凋亡具有保护作用^[7],然而是否通过PERK/eIF2 α /ATF4/CHOP通路减轻ROS/ERS引起的成骨细胞凋亡尚未涉及。本研究采用过氧化氢(hydrogen peroxide, H₂O₂)诱导UMR-106细胞形成ROS/ERS模型,观察健骨颗粒含药血清对ROS、细胞凋亡率和PERK/eIF2 α /ATF4/CHOP通路的影响,探讨健骨颗粒保护ROS/ERS的UMR-106细胞模型的潜在机制,为PMOP的临床治疗提供实验支持。

1 材料与方法

1.1 实验动物

SPF级6周龄雄性SD大鼠40只,购自浙江省医学科学院[生产许可证号:SCXK(闽)1908140006]。实验动物饲养于福建中医药大学实验动物中心SPF级实验室[使用许可证:SYXK(闽)2019-0007],实验前适应性喂养1周,本研究已通过福建中医药大学动物伦理委员会审核会批准通过[批准号:福中医伦理审字[2018]第(038)号]。

1.2 实验细胞

UMR-106成骨样细胞株购自中国科学院典型培养物保藏委员会细胞库(目录号:TCR11)。

1.3 主要试剂与仪器

1.3.1 实验药物 健骨颗粒由淫羊藿、山茱萸、党参、淮山药、煅狗骨等组成,购自福建省同春药业股份有限公司(每克颗粒剂含原生药2.9g),由福建省中医药科学院内试车间依照课题组制剂工艺标准煎煮浓缩,制备成健骨颗粒浸膏,-20℃冰箱保存。

1.3.2 主要实验试剂 DMEM培养基、PBS、0.25%胰蛋白酶均购自于美国Sigma公司;FBS购自于美国Gibco公司;GSK2606414购自于美国APEX BIO公司;活性氧分析试剂盒、Annexin V-FITC/PI凋亡检测试剂盒均购自于江苏凯基生物技术股份有限公司;HiScript Q RT SuperMix for qPCR、AceQ qPCR SYBR Green Master Mix均购自于南京诺唯赞生物科技股份有限公司;PERK一抗购自于美国Cst公司;eIF2 α 、ATF4、CHOP、 β -actin一抗均购自于Prontein-tech公司;Capase-12一抗购自于北京博奥森生物技术有限公司;Fluo-3 AM购自于株式会社日本同仁化学研究所。

1.3.3 主要实验仪器 CO₂恒温培养箱购自于香港力康公司;低速离心机购自于德国Eppendorf公司;ELx800全自动酶标仪购自于美国Thermo Fisher Scientific公司;倒置相差显微镜购自于日本TKO光学仪器株式会社;激光共聚焦扫描显微镜购自于卡尔蔡司光学有限公司;流式细胞仪购自于美国BD公司;7500 Fast实时荧光定量PCR仪购自于美国Life technologies公司;化学发光成像系统购自于美国Bio-Rad公司。

1.4 实验方法

1.4.1 生理盐水血清和健骨颗粒含药血清制备 将40只SD大鼠采用随机数字表法分为生理盐水血清组和健骨颗粒含药血清组,每组20只。生理盐水组采用生理盐水灌胃,健骨颗粒灌胃剂量根据人和大鼠的体表面积进行换算,按照7.8 g/(kg·d)生药量连续灌胃7d,最后一次灌胃后2h后腹主动脉取血,静置4h后3 000 r/min离心15 min取血清,56℃水浴30 min灭活补体,0.22 μ mol/L过滤器过滤后分装,存储于-80℃超低温冰箱。

1.4.2 细胞培养和分组干预 选用UMR-106细胞,采用10% FBS、100 μ g/mL青霉素和100 μ g/mL链霉素的DMEM培养基,培养于5% CO₂ 37℃恒温的细胞培养箱中。将细胞随机分为阴性对照组(NC

组)、模型组(H₂O₂组)、健骨颗粒组(H₂O₂+JG组)和阳性对照组(H₂O₂+GSK2606414组)。NC组和H₂O₂组采用10%生理盐水血清干预12 h, H₂O₂+JG组采用10%健骨颗粒含药血清干预12 h, H₂O₂+GSK2606414组采用0.03 μmol/L的GSK2606414和10%生理盐水血清干预12 h,除NC组外,其余各组在不更换新培养基的情况下,再分别加入10 μmol/L H₂O₂干预12 h制备ERS模型。

1.4.3 CCK8法筛选GSK2606414最佳干预浓度 将UMR-106细胞按1×10⁴个/孔接种在96孔板中并培养24 h,采用不同浓度(0、0.01、0.02、0.03、0.04、0.05 μmol/L)的GSK2606414处理细胞,每个浓度重复6次,孵育12 h,每孔加入CCK8 10 μL,37 °C孵育1 h,酶标仪检测450 nm处吸光度,选取对UMR-106细胞活力没有影响的最大浓度作为GSK2606414的最佳干预浓度进行后续实验。

1.4.4 激光共聚焦显微镜观察细胞内GRP78和Caspase-12荧光表达情况 将UMR-106细胞按8×10⁴个/mL接种至共聚焦皿,分别培养24 h,弃液,PBS洗涤3 min×3次,4%多聚甲醛固定30 min,PBS洗涤;3% H₂O₂室温孵育10 min,PBS洗涤3 min×3次;SABC室温孵育10 min,PBS洗涤;封闭液孵育1 h,弃液,分别加入GRP78(1:1 000)和Caspase-12(1:1 000)一抗4 °C孵育过夜;弃液,PBS洗涤,避光加入1:1 000荧光二抗室温孵育1 h;PBS洗净,加入500 μL DAPI孵育10 min,PBS洗净后激光共聚焦显微镜观察并拍摄。

1.4.5 DCFH-DA法测定细胞内ROS含量 将UMR-106细胞按8×10⁴个/mL接种至共聚焦皿,分别培养24 h,弃液,用DMEM洗涤3次;按照1:1 000加入DCFH-DA荧光探针,37 °C避光孵育20 min;激光共聚焦显微镜拍摄,ImageJ分析实验结果。

1.4.6 激光共聚焦显微镜观察细胞内钙离子实时动态变化 将UMR-106细胞按8×10⁴个/mL接种至共聚焦皿,培养24 h,弃液,Hank's平衡盐溶液(HBSS溶液)洗涤5 min×3次,加入30 μmol/L Fluo-3 AM工作液1.25 μL,再加入0.05% Pluronic F-127工作液1.25 μL,轻晃混匀,避光37 °C孵育30 min;弃液,HBSS溶液洗涤3 min,加入500 μL HBSS,再加入5 μL Hoechst33342孵育10 min;弃液,HBSS溶液洗涤5 min×3次。根据组别分别滴加10%生理盐水血清及10 μmol/L H₂O₂,激光共聚焦显微镜拍摄,设置拍摄视频时长约40 min,ZEN软件分析。

1.4.7 Annexin V-FITC/PI检测细胞凋亡率 UMR-

106细胞按2×10⁵个/孔接种于6孔板,分组干预,弃液,PBS洗涤,每孔加入200 μL不含EDTA胰酶消化2 min,加入完全培养基终止消化,收集细胞悬液至15 mL离心管,2 000 r/min离心3 min;弃液,PBS洗涤,2 000 r/min离心3 min;每管加入500 μL Binding Buffer,轻柔吹打混匀移入流式管,每管加入5 μL Annexin V-FITC和5 μL PrPidium Iodide充分混匀,避光孵育15 min,流式细胞仪上机检测,FLOWJO软件分析数据,实验重复3次以上进行统计。

1.4.8 qPCR检测细胞ERS标志基因GRP78及PERK通路关键指标mRNA转录水平 分别收集4组细胞,加入TriZol 1 mL充分混匀,静置10 min;加入氯仿200 μL,震荡30 s混匀,4 °C 12 000 r/min离心20 min;取400 μL上清至新EP管中,再加入400 μL异丙醇,充分混匀后冰上静置15 min,放入离心机中4 °C 12 000 r/min离心20 min;弃液,加入75%乙醇1 mL,4 °C 7 500 r/min离心5 min,弃液,加入20 μL DEPC溶解总RNA;nanodrop 2000分光光度计检测OD₂₆₀/OD₂₈₀值。HiScript QRT SuperMix将RNA逆转录成cDNA,AceQ-qPCR SYBR Green Master Mix配置qPCR反应体系,条件如下:95 °C 10 s和60 °C 30 s共40个循环,95 °C 15 s、60 °C 60 s、95 °C 15 s共1个循环得到溶解曲线,GAPDH作为内参,2^{-ΔΔCt}计算目的基因相对表达量。引物序列见表1。

表1 引物序列

Table 1 Primer sequence

基因名称	引物序列(5'→3')
GRP78	F:5'CGTCGTATGTGGCCTTCACT3'
	R:5'ATTCCAAGTGCCTCCGATGA3'
PERK	F:5'ACCTCAAGCCTTCCAACATATTC3'
	R:5'TACTGTCTGCTCTTCTTCATCCT3'
eIf2α	F:5'GCATTCTTCGCCATGTTGCT3'
	R:5'AGGCACCATATCCAGGTCTCT3'
ATF4	F:5'GCCTGACTCTGCTGCTTATATTAC3'
	R:5'ACGAGGAACACCTGGAGAAG3'
CHOP	F:5'ACGGAAACAGAGTGGTCAGT3'
	R:5'CGCTCGATTCCTGCTTGAG3'
GAPDH	F:5'ACGGCAAGTTCAACGGCACAG3'
	R:5'GAAGACGCCAGTAGACTCCACGAC3'

1.4.9 Western blot检测细胞ERS标志蛋白GRP78及PERK通路关键指标蛋白含量 分别收集4组细胞,弃液,PBS洗涤,加入100 μL RIPA裂解液、1 μL PMSF和1 μL磷酸酶抑制剂,冰上裂解30 min,4 °C 12 000 r/min离心18 min,取蛋白上清,按照1:4比

例加入 25 μ L 5 \times Loading Buffer,充分混匀,95 $^{\circ}$ C 变性 5 min,-80 $^{\circ}$ C 保存。采用 6~10% SDS-PAGE 电泳,湿转至 0.22 μ m PVDF 膜上,QuickBlock™快速封闭液室温孵育 5 min,分别采用 GRP78(1:1 000)、PERK(1:1 000)、eIF2 α (1:1 000)、ATF4(1:1 000)、CHOP(1:1 000)和 β -actin(1:5 000),一抗 4 $^{\circ}$ C 孵育过夜,TBST 洗涤,1:10 000 二抗室温孵育 1 h,TBST 洗涤,滴加显影液曝光成像,以 β -actin 作为内参,计算目标蛋白相对表达量。

1.5 统计学方法

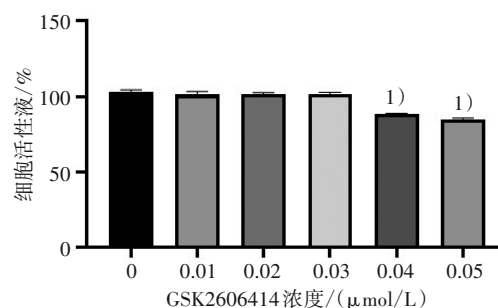
实验数据采用 SPSS 25.0 软件统计分析。数据符合正态分布以($\bar{x}\pm s$)表示,组间比较采用单因素方差分析,方差齐时用 LSD-*t* 法,方差不齐时用 Games-Howell 法。数据不符合正态分布时采用非参数检验法。以 $P<0.05$ 表示差异有统计学意义。

2 结果

2.1 GSK2606414 抑制剂的最佳干预浓度

与 0 μ mol/L 的空白对照组相比,0.01、0.02 和 0.03 μ mol/L GSK2606414 处理后细胞活力没有显著变化,0.04、0.05 μ mol/L GSK2606414 可观察到细胞活力显著降低($P<0.01$)。见图 1。结果表明 GSK2606414 干预 UMR-106 细胞 12 h 后对细胞活力没有影响的最大浓度为 0.03 μ mol/L,故使用该浓度

作为后续 H₂O₂+GSK2606414 组的实验干预条件。



注:与 0 μ mol/L 相比,1) $P<0.01$ 。

Note: Compared with the 0 μ mol/L, 1) $P<0.01$.

图 1 不同浓度 GSK2606414 对 UMR-106 细胞活力的比较
Figure 1 Comparison different concentrations of GSK2606414 on the viability of UMR-106 cells

2.2 NC 组和 H₂O₂ 组 GRP78 和 Caspase-12 蛋白荧光表达比较

本实验沿用课题组前期成熟的体外细胞氧化应激造模条件,采用 10 μ mol/L H₂O₂ 干预 UMR-106 细胞 12 h 诱导氧化应激^[8]。免疫荧光染色观察 ERS 标志物蛋白 GRP78 和 ERS 细胞凋亡指标 Caspase-12 的表达水平。结果显示:与 NC 组相比,H₂O₂ 处理后 GRP78 和 Caspase-12 的荧光强度显著增加,表明 H₂O₂ 诱导 UMR-106 细胞 ROS/ERS 模型的成功建立。见图 2。

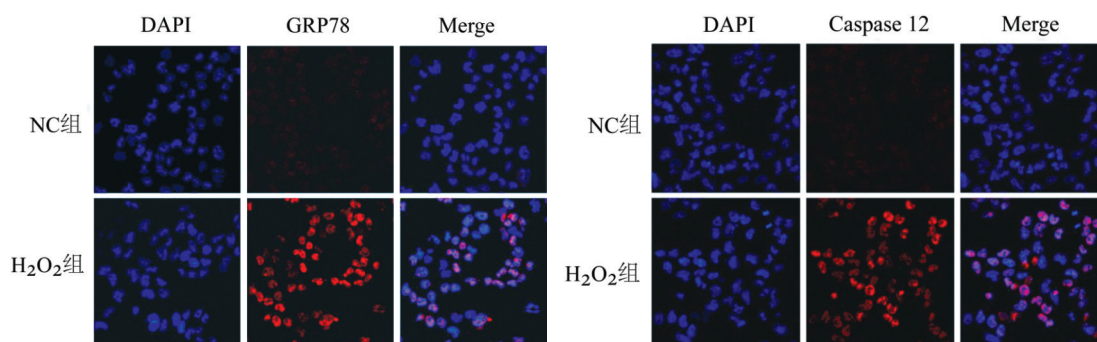


图 2 UMR-106 细胞 GRP78 和 Caspase-12 蛋白荧光强度比较($\times 400$)

Figure 2 Comparison of fluorescence intensity of GRP78 and Caspase-12 of UMR-106 cells ($\times 400$)

2.3 NC 组和 H₂O₂ 组钙离子实时动态变化比较

Fluo 3-AM 检测细胞内钙离子实时动态变化,结果显示:NC 组细胞内钙离子流随时间推移无明显变化,处于相对稳定状态;H₂O₂ 处理后 H₂O₂ 组荧光强度和钙离子流速随时间推移而增加,进一步表明 H₂O₂ 诱导 UMR-106 细胞 ROS/ERS 模型的成功建立。见图 3。

2.4 NC 组和 H₂O₂ 组 ROS 含量比较

线粒体是细胞内 ROS 的主要来源,DCFH-DA 探针证实 H₂O₂ 处理后 UMR-106 细胞内 ROS 含量显著升高($P<0.01$);健骨颗粒和 GSK2606414 干预后细胞内 ROS 含量显著降低($P<0.01$)。见图 4。结果表明健骨颗粒可抑制 ROS/ERS 模型细胞中 ROS 的生成。

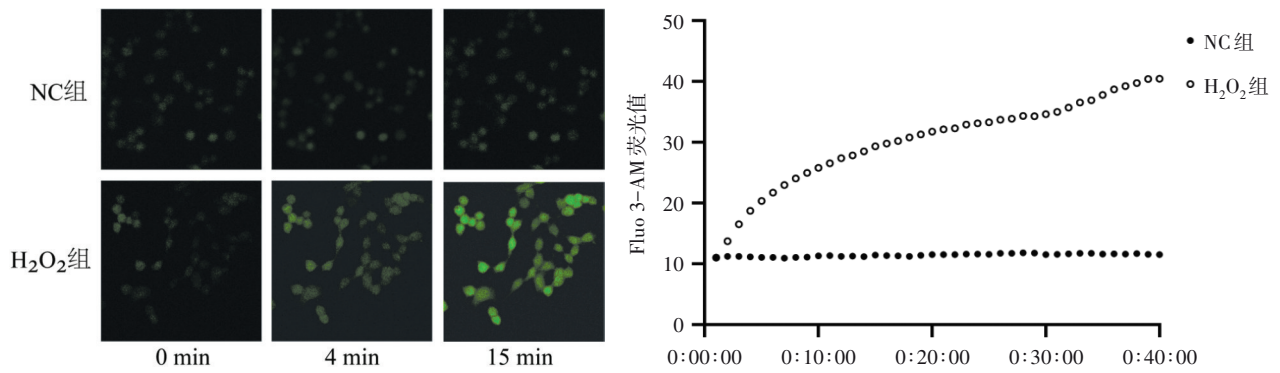
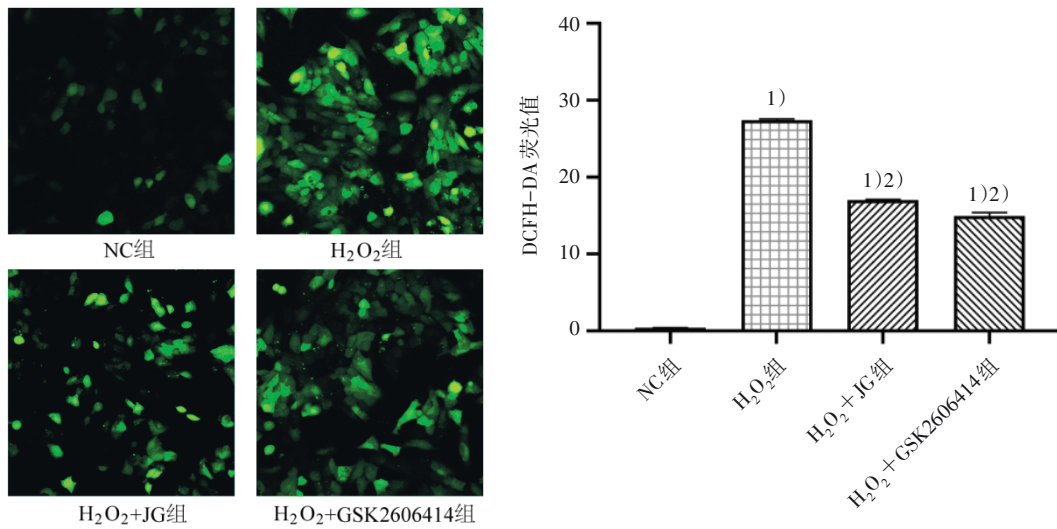


图3 细胞钙离子实时动态变化比较(×400)

Figure 3 Comparison of real-time dynamic changes in cellular calcium ions (×400)



注:与NC组比较,1) $P < 0.01$;与H₂O₂组比较,2) $P < 0.01$ 。

Note: Compared with the negative control group, 1) $P < 0.01$; compared with the H₂O₂ group, 2) $P < 0.01$.

图4 ROS含量比较(×400)

Figure 4 Comparison of ROS content (×400)

2.5 4组细胞晚期凋亡率比较

与NC组比较,H₂O₂组细胞晚期凋亡率升高($P < 0.01$),健骨颗粒和GSK2606414干预后细胞晚期凋亡率均有所下降($P < 0.05$)。见图5。

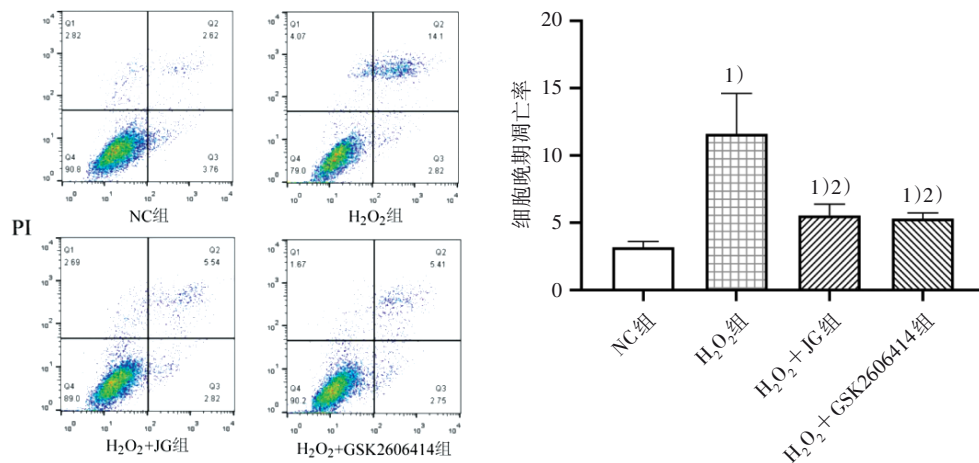
2.6 4组PERK/eIF2 α /ATF4/CHOP通路关键基因mRNA转录水平比较

与NC组相比,H₂O₂组GRP78、PERK、eIF2 α 、ATF4和CHOP mRNA转录水平显著增高($P < 0.01$);与H₂O₂相比,健骨颗粒和GSK2606414干预后GRP78、

PERK、eIF2 α 、ATF4和CHOP mRNA转录水平均降低($P < 0.01$)。见图6。

2.7 4组PERK/eIF2 α /ATF4/CHOP通路关键蛋白相对表达量比较

与NC组相比,H₂O₂组GRP78、PERK、eIF2 α 、ATF4和CHOP蛋白相对表达量显著增高($P < 0.01$);与H₂O₂组相比,健骨颗粒和GSK2606414干预后GRP78、PERK、eIF2 α 、ATF4和CHOP蛋白相对表达量均降低($P < 0.05$)。见图7。

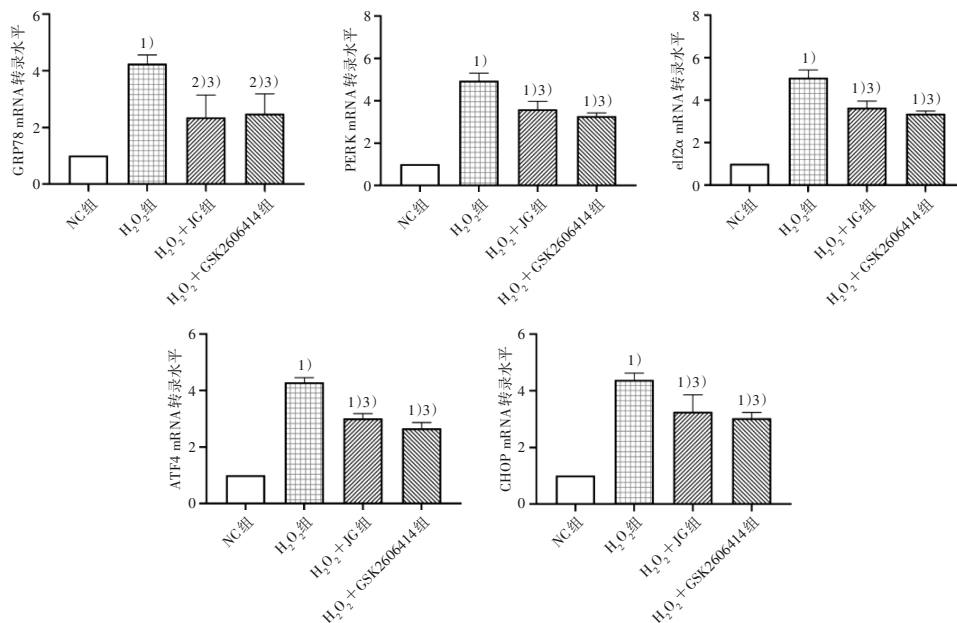


注:与NC组相比,1) $P < 0.01$;与H₂O₂组相比,2) $P < 0.05$ 。

Note: Compared with the negative control group, 1) $P < 0.01$; Compared with H₂O₂ exposure group, 2) $P < 0.05$.

图5 4组细胞晚期凋亡率比较

Figure 5 Comparison of advanced cell apoptosis rates in four groups



注:与NC组比较,1) $P < 0.01$, 2) $P < 0.05$;与H₂O₂组比较,3) $P < 0.01$ 。

Note: Compared with the negative control group, 1) $P < 0.01$, 2) $P < 0.05$; compared with the H₂O₂ group, 3) $P < 0.01$.

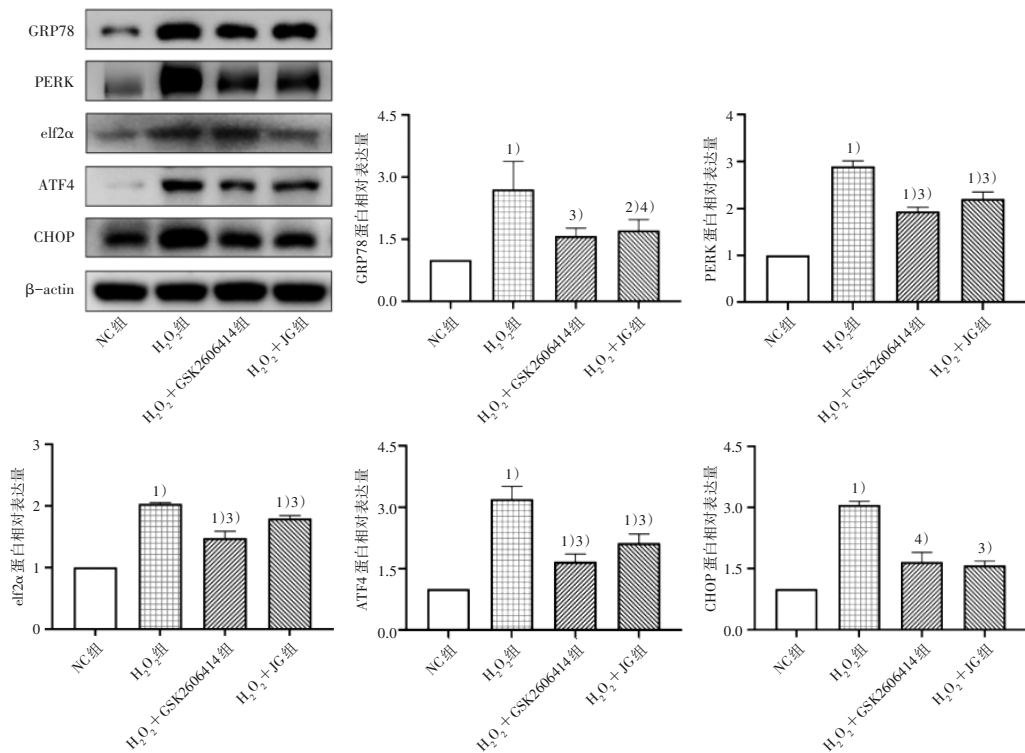
图6 4组PERK/eIF2 α /ATF4/CHOP通路关键基因mRNA转录水平比较

Figure 6 Comparison of mRNA expression level of key genes in the PERK/eIF2 α /ATF4/CHOP pathway

3 讨论

PMOP发病率显著高于老年性骨质疏松症,严重影响中老年女性的生活质量。现阶段治疗药物分为四大类:抑制骨吸收药物(雌激素类、选择性雌激素受体调节剂、双膦酸盐类和降钙素),促进骨形成药物(甲状旁腺激素等),双重作用药物(雷尼酸锶等)和骨矿化促进剂(钙剂、维生素D)。虽然雌激

素水平急剧降低是PMOP的主要病因,然而雌激素替代治疗可引起子宫癌和乳腺癌的风险性增加^[9]。双膦酸盐类抑制骨吸收量的同时新生骨量和质量相应减少,可能引起颌骨坏死等严重不良反应^[10]。甲状旁腺激素(特立帕肽)的最长持续使用时间是2年。中医药因其独特优势受到医患的广泛关注^[11-13],进一步明确其作用机制势在必行。



注:与NC组比较,1) $P < 0.01$, 2) $P < 0.05$;与H₂O₂比较,3) $P < 0.01$, 4) $P < 0.05$ 。

Note: Compared with the negative control group, 1) $P < 0.01$, 2) $P < 0.05$; compared with the H₂O₂ group, 3) $P < 0.01$, 4) $P < 0.05$.

图7 4组PERK/eIF2α/ATF4/CHOP通路关键蛋白相对表达量比较

Figure 7 Comparison of expression level of key proteins in the PERK/eIF2α/ATF4/CHOP pathway in four groups

ROS包括氧和含氧的高反应活性分子,例如H₂O₂、超氧阴离子(O²⁻)和羟基自由基(·OH)等,氧化应激可损伤成骨细胞的细胞成分,是骨质流失的致病因素之一^[14]。本实验采用H₂O₂制备细胞模型,其直接攻击维持蛋白折叠酶活性所必需的游离巯基,内质网腔内蛋白质被氧化修饰,触发ERS,ERS是重要的细胞自我防御机制,适当的ERS有助于成骨分化,然而持续、过度的ERS抑制成骨分化并诱导其凋亡,ERS在PMOP的发生和发展中起重要作用^[15-16]。实验结果显示:10 μmol/L H₂O₂干预UMR-106细胞12 h,在ROS水平达到峰值的同时GRP78和Caspase-12表达水平显著增强,细胞内钙离子内流速度随时间推移显著加快,并且细胞凋亡率显著增加,以上结果均提示H₂O₂引起ERS细胞凋亡的发生,即ROS/ERS模型构建成功。

内质网是细胞的钙库,Ca²⁺是重要的第二信使,参与细胞增殖、分化和凋亡等生物学过程^[17]。同时内质网的蛋白质合成、折叠、组装和钙离子贮存等功能是细胞命运决定的关键因素。GRP78是伴侣蛋白,在蛋白质的折叠和组装中发挥关键作用,负

责UPR迅速启动,并作为内质网稳态的主要调节因子。PERK/eIF2α/ATF4/CHOP信号通路是调控ERS的3个主要通路之一^[18],同时也是调控成骨细胞分化和骨形成的主要信号通路之一^[19]。

PERK是内质网膜上的跨膜蛋白,PERK基因敲除小鼠出现骨骼缺陷包括成骨细胞数量不足、成骨细胞分化矿化受损、I型胶原分泌减少、骨质疏松和异常致密骨发育等^[20-21];在生理条件下PERK处于无活性状态,与内质网中含量最丰富的分子伴侣GRP78结合形成稳定的复合物,UPR时PERK与GRP78解离,游离GRP78与内质网中蛋白结合,增强内质网的蛋白质折叠能力,缓解ERS;然而反应是有限的,当未折叠或错误折叠蛋白质过度堆积,机体为保护其他细胞的正常功能启动凋亡途径^[4,22]。游离PERK引起下游eIF2α磷酸化导致蛋白翻译水平整体下降或者停止,但诱导ATF4的优先翻译和合成,ATF4也是成骨细胞的关键调控因子^[23-25],进而激活其下游转录因子C/EBP同源蛋白CHOP的转录,CHOP是启动应激凋亡通路的关键蛋白,最终导致细胞凋亡。本实验中H₂O₂处理后PERK、eIF2α、

ATF4和CHOP mRNA转录水平和蛋白相对表达量均显著增加,表明该信号通路在UMR-106细胞的ERS凋亡中起重要作用。

SU等^[26]发现叶酸可能通过抑制ERS减少成骨细胞凋亡,MENG等^[27]发现褪黑素通过eIF2 α /ATF4通路的激活诱导hFOB 1.19细胞凋亡,而POSTN可能通过抑制eIF2 α /ATF4通路保护成骨细胞;LI等^[28]发现OVX小鼠中增强eIF2 α 磷酸化可引起骨密度和骨体积分数的增加。GSK2606414是PERK的选择性抑制剂,可通过抑制PERK磷酸化和降低PERK含量,阻碍下游ATF4和CHOP的激活,广泛用于验证PERK信号通路在各种疾病模型中的作用^[29]。本实验中GSK2606414干预后ROS含量和细胞凋亡率均显著降低,PERK、eIF2 α 、ATF4和CHOP mRNA转录水平和蛋白相对表达量出现不同程度的下降;上述结果表明减轻ERS可能在保护成骨细胞对抗PMOP中发挥关键作用。

健骨颗粒是治疗PMOP的验方,主要由淫羊藿、山茱萸、党参、淮山药和煅狗骨等组成,具有补肾健脾、强筋健骨之功效,临床效果显著。课题组前期系列研究发现:健骨颗粒可能通过调节与成骨细胞分化相关的6个靶蛋白相对表达量,增强去卵巢大鼠成骨细胞分化能力以发挥治疗作用^[30];通过p38MAPK信号通路调控成骨细胞增殖^[31];健骨颗粒氯仿萃取部位调控BMP2/Smad1/Runx2/Osterix通路促进成骨细胞分化^[32-33]。本实验结果显示:健骨颗粒干预可显著降低ROS含量和细胞凋亡率,PERK、eIF2 α 、ATF4和CHOP mRNA转录水平和蛋白相对表达量不同程度降低;提示健骨颗粒可通过调控PERK/eIF2 α /ATF4/CHOP信号通路减轻过度的ERS,从而降低UMR-106细胞凋亡率,发挥成骨细胞保护作用。

综上所述,调控PERK/eIF2 α /ATF4/CHOP信号通路可能是健骨颗粒治疗PMOP的潜在作用机制之一;但本实验仅限于体外细胞实验,存在一定的局限性,后续还需要进一步的动物实验来验证该作用机制。

参考文献

- [1] KANIS J A. Diagnosis of osteoporosis and assessment of fracture risk [J]. *Lancet*, 2002, 359(9321): 1929-1936.
- [2] ALMEIDA M, LAURENT M R, DUBOIS V, et al. Estrogens and androgens in skeletal physiology and pathophysiology [J]. *Physiol Rev*, 2017, 97(1): 135-187.
- [3] CHANDRA A, RAJAWAT J. Skeletal aging and osteoporosis: mechanisms and therapeutics [J]. *Int J Mol Sci*, 2021, 22(7): 3553.
- [4] LI J, YANG S, LI X L, et al. Role of endoplasmic reticulum stress in disuse osteoporosis [J]. *Bone*, 2017, 97: 2-14.
- [5] ZHONG M L, WU Z Y, CHEN Z X, et al. Advances in the interaction between endoplasmic reticulum stress and osteoporosis [J]. *Biomedecine Pharmacother*, 2023, 165: 115134.
- [6] GUO J C, REN R Y, SUN K, et al. PERK signaling pathway in bone metabolism: friend or foe? [J]. *Cell Prolif*, 2021, 54(4): e13011.
- [7] 李异龙, 吴银生, 林燕萍. 健骨颗粒含药血清对肿瘤坏死因子 α 诱导大鼠成骨细胞凋亡的影响[J]. *中国组织工程研究与临床康复*, 2009, 13(7): 1227-1231.
LI Y L, WU Y S, LIN Y P. Effect of serum containing Jiangu Granule on apoptosis of osteoblasts induced by tumor necrosis factor α in rats [J]. *Chin J Tissue Eng Res*, 2009, 13(7): 1227-1231.
- [8] 孙攀. Nrf2通路介导抗氧化应激调控去卵巢大鼠骨稳态机制及健骨颗粒干预作用研究[D]. 福州: 福建中医药大学, 2021: 22-25.
SUN P. The mechanism of Nrf2 signaling pathway regulating bone homeostasis in ovariectomized rats through antioxidant stress and the treatment of Jiangu Granules [D]. Fuzhou: Fujian University of Traditional Chinese Medicine, 2021: 22-25.
- [9] PAN M J, PAN X Y, ZHOU J, et al. Update on hormone therapy for the management of postmenopausal women [J]. *Biosci Trends*, 2022, 16(1): 46-57.
- [10] JENSEN P R, ANDERSEN T L, CHAVASSIEUX P, et al. Bisphosphonates impair the onset of bone formation at remodeling sites [J]. *Bone*, 2021, 145: 115850.
- [11] LIANG H T, WANG O, CHENG Z F, et al. Jintiang combined with alfacalcidol improves muscle strength and balance in primary osteoporosis: a randomized, double-blind, double-dummy, positive-controlled, multicenter clinical trial [J]. *J Orthop Translat*, 2022, 35: 53-61.
- [12] LUO M H, ZHAO J L, XU N J, et al. Comparative efficacy of Xianling Gubao capsules in improving bone mineral density in postmenopausal osteoporosis: a network meta-analysis [J]. *Front Endocrinol*, 2022, 13: 839885.
- [13] REN Z Q, WANG Y F, AO G F, et al. Overall adjustment acupuncture for postmenopausal osteoporosis (PMOP): a study protocol for a randomized sham-controlled trial [J]. *Trials*, 2020, 21(1): 465.
- [14] YANG Y H, LI B, ZHENG X F, et al. Oxidative damage to osteoblasts can be alleviated by early autophagy through the endoplasmic reticulum stress pathway: implications for the treatment of osteoporosis [J]. *Free Radic Biol Med*, 2014, 77: 10-20.
- [15] BEZAMAT M, DEELEY K, KHALIQ S, et al. Are mTOR and endoplasmic reticulum stress pathway genes associated with oral and bone diseases? [J]. *Caries Res*, 2019, 53(3): 235-241.
- [16] SUZUKI R, FUJIWARA Y, SAITO M, et al. Intracellular accumulation of advanced glycation end products induces osteoblast apoptosis via endoplasmic reticulum stress [J]. *J Bone Miner Res*, 2020, 35(10): 1992-2003.

- [17] CARRERAS-SUREDA A, PIHÁN P, HETZ C. Calcium signaling at the endoplasmic reticulum: fine-tuning stress responses [J]. *Cell Calcium*, 2018, 70:24–31.
- [18] BALSÀ E, SOUSTEK M S, THOMAS A, et al. ER and nutrient stress promote assembly of respiratory chain super complexes through the PERK-eIF2 α axis [J]. *Mol Cell*, 2019, 74(5): 877–890. e6.
- [19] YANG S Y, HU L H, WANG C L, et al. PERK-eIF2 α -ATF4 signaling contributes to osteogenic differentiation of periodontal ligament stem cells [J]. *J Mol Histol*, 2020, 51(2): 125–135.
- [20] WEI J W, SHENG X Y, FENG D R, et al. PERK is essential for neonatal skeletal development to regulate osteoblast proliferation and differentiation [J]. *J Cell Physiol*, 2008, 217(3): 693–707.
- [21] ZHANG P C, MCGRATH B, LI S A, et al. The PERK eukaryotic initiation factor 2 alpha kinase is required for the development of the skeletal system, postnatal growth, and the function and viability of the pancreas [J]. *Mol Cell Biol*, 2002, 22(11): 3864–3874.
- [22] IURLARO R, MUÑOZ-PINEDO C. Cell death induced by endoplasmic reticulum stress [J]. *FEBS J*, 2016, 283(14): 2640–2652.
- [23] YANG X L, MATSUDA K, BIALEK P, et al. ATF4 is a substrate of RSK2 and an essential regulator of osteoblast biology; implication for Coffin-Lowry Syndrome [J]. *Cell*, 2004, 117(3): 387–398.
- [24] ST-ARNAUD R, HEKMATNEJAD B. Combinatorial control of ATF4-dependent gene transcription in osteoblasts [J]. *Ann N Y Acad Sci*, 2011, 1237: 11–18.
- [25] ZHANG Y, LIN T H, LIAN N, et al. Hop2 interacts with ATF4 to promote osteoblast differentiation [J]. *J Bone Miner Res*, 2019, 34(12): 2287–2300.
- [26] SU S, ZHANG D, LIU J J, et al. Folate ameliorates homocysteine-induced osteoblast dysfunction by reducing endoplasmic reticulum stress-activated PERK/ATF-4/CHOP pathway in MC3T3-E1 cells [J]. *J Bone Miner Metab*, 2022, 40(3): 422–433.
- [27] MENG X T, ZHU Y, TAO L, et al. Periostin has a protective role in melatonin-induced cell apoptosis by inhibiting the eIF2 α -ATF4 pathway in human osteoblasts [J]. *Int J Mol Med*, 2018, 41(2): 1003–1012.
- [28] LI J, LI X L, LIU D Q, et al. eIF2 α signaling regulates autophagy of osteoblasts and the development of osteoclasts in OVX mice [J]. *Cell Death Dis*, 2019, 10(12): 921.
- [29] GUO J C, REN R Y, SUN K, et al. PERK controls bone homeostasis through the regulation of osteoclast differentiation and function [J]. *Cell Death Dis*, 2020, 11(10): 847.
- [30] LIN H M, ZHANG W, XU Y S, et al. 4D label-free quantitative proteomics analysis to screen potential drug targets of Jiangu Granules treatment for postmenopausal osteoporotic rats [J]. *Front Pharmacol*, 2022, 13: 1052922.
- [31] 吴银生, 林煜, 卢天祥, 等. p38MAPK通路在健骨颗粒促成骨细胞早期分化中的作用 [J]. *福建中医药大学学报*, 2010, 20(6): 30–34.
- WU Y S, LIN Y, LU T X, et al. The role of p38MAPK pathway in the early differentiation of bone cells promoted by Jiangu Granule [J]. *Fujian University of Traditional Chinese Medicine*, 2010, 20(6): 30–34.
- [32] 陈翔, 林燕萍, 贾晓康, 等. 健骨颗粒乙酸乙酯萃取部位对卵巢切除大鼠骨质量的影响 [J]. *中华中医药杂志*, 2018, 33(11): 4925–4928.
- CHEN X, LIN Y P, JIA X K, et al. Effect of ethyl acetate extract of Jiangu Granules on bone quality in ovariectomized rats [J]. *China J Tradit Chin Med Pharm*, 2018, 33(11): 4925–4928.
- [33] 周芬, 孙雨晴, 孙攀, 等. 基于BMP2/Smad1/Runx2/Osterix信号通路探讨健骨颗粒氯仿萃取部位对体外成骨细胞分化的影响 [J]. *康复学报*, 2022, 32(3): 224–231.
- ZHOU F, SUN Y Q, SUN P, et al. Based on BMP2/Smad1/Runx2/Osterix signal pathway, the effect of chloroform extraction site of Jiangu Granule on osteoblast differentiation *in vitro* was discussed [J]. *Rehabil Med*, 2022, 32(3): 224–231.

Jiangu Granules Regulates Endoplasmic Reticulum Stress-Induced Apoptosis in UMR-106 Cells by Modulating the PERK/eIF2 α /ATF4/CHOP Pathway

CHEN Sainan^{1,2,3}, ZHOU Fen^{1,2,4}, HUANG Yunmei^{1,2}, LIN Yanping^{1,2*}

¹ Academy of Integrative Medicine, Fujian University of Traditional Chinese Medicine, Fuzhou, Fujian 350122, China;

² Fujian Provincial Key Laboratory of Integrative Medicine on Geriatrics, Fuzhou, Fujian 350122, China;

³ Key Research Section of Osteoporosis Syndrome Genomics, Fujian Academy of Chinese Medical Sciences, Fuzhou, Fujian 350003, China;

⁴ Periodical Press, Fujian University of Traditional Chinese Medicine, Fuzhou, Fujian 350122, China

*Correspondence: LIN Yanping, E-mail: linyanping1966@163.com

ABSTRACT Objective To observe and analyze the mechanism by which Jiangu Granules containing serum alleviate endoplasmic reticulum stress (ERS)-induced apoptosis in UMR-106 osteoblast-like cells. **Methods** UMR-106 osteoblast-like cells were selected for the study, and various concentrations (0, 0.01, 0.02, 0.03, 0.04, 0.05 $\mu\text{mol/L}$) of GSK2606414 (PERK inhibitor) were employed to intervene in the cells. The optimal intervention concentration of GSK2606414 was determined using the CCK8 method. UMR-106 cells exhibiting favorable growth status were randomly allocated into four groups: negative control group (NC group), model group (H_2O_2 group), Jiangu Granules group (H_2O_2 +JG group), and positive control group (H_2O_2 +GSK2606414 group). The NC and H_2O_2 groups were intervened with 10% saline serum for a duration of 12 hours. The H_2O_2 +JG group was intervened with 10% Jiangu Granules containing serum for 12 hours, while the H_2O_2 +GSK2606414 group underwent intervention with 0.03 $\mu\text{mol/L}$ GSK2606414 and 10% normal saline serum, for 12 hours. The last three groups were supplemented with 10 $\mu\text{mol/L}$ H_2O_2 solution

without altering the new culture medium for 12 hours. The fluorescence expression of GRP78 and Caspase-12 in cells of the NC and H₂O₂ groups was observed using laser confocal microscopy. Intracellular ROS content was detected using DCFH-DA. The real-time dynamic changes of intracellular calcium ions were observed using laser confocal microscopy to determine whether the ROS/ERS model was constructed. Late apoptosis rate was determined using Annexin V-FITC/PI in the four groups. Additionally, mRNA transcription level and protein expression of ERS related markers GRP78, PERK, eIF2 α , ATF4, and CHOP were detected using qPCR and Western blot methods. **Results** In comparison to the 0 μ mol/L group, it was found that 0.03 μ mol/L of GSK2606414 had no impact on cell viability after 12 hours of intervention in UMR-106 cells, and this concentration was chosen for subsequent experiments. Compared with the NC group, the H₂O₂ group showed a significant increase in ROS content ($P < 0.01$). The protein fluorescence expression level of GRP78 and Caspase-12 exhibited a significant increase. Additionally, the intracellular calcium ion flow rate demonstrated an accelerated and continuous increase, indicating the successful establishment of the H₂O₂ induced ROS/ERS model in UMR-106 cells. In comparison to the NC group, the apoptosis rate in the H₂O₂ group displayed a significant increase ($P < 0.05$). Furthermore, the mRNA transcription level and protein expression level of ATF4 and CHOP, as well as GRP78, PERK, and eIF2 α , exhibited a significant increase ($P < 0.01$). Compared with the H₂O₂ group, the H₂O₂+JG group and the H₂O₂+GSK2606414 group showed a significant decrease in the ROS content ($P < 0.01$) and apoptosis rate ($P < 0.05$). The mRNA transcription level ($P < 0.05$) and protein expression ($P < 0.01$) of GRP78, PERK, eIF2 α , ATF4, CHOP were significantly down-regulated. **Conclusion** These findings suggest that Jiangu Granules can alleviate endoplasmic reticulum stress and reduce apoptosis in osteoblast-like cells through the PERK/eIF2 α /ATF4/CHOP signaling pathway, thereby potentially playing a role in the prevention and treatment of postmenopausal osteoporosis.

KEY WORDS postmenopausal osteoporosis; endoplasmic reticulum stress; Jiangu Granules; PERK/eIF2 α /ATF4/CHOP signaling pathway; osteoblast apoptosis

DOI:10.3724/SP.J.1329.2024.01006

(上接第33页)

Influence of Interactive Scalp Acupuncture Combined with Upper Limb Exoskeleton Robot on Upper Limb Function in Stroke Patients

WANG Zihao¹, HU Chuan², ZHANG Haiquan², WANG Xin^{*}

¹ Shandong Sport University, Jinan, Shandong 250102, China;

² Shandong Provincial Third Hospital, Affiliated to Shandong University, Jinan, Shandong 250031, China

*Correspondence: WANG Xin, E-mail: 18530915@qq.com

ABSTRACT Objective Based on the central-peripheral-central-closed loop theory, the study aimed to investigate the influence of interactive scalp acupuncture combined with upper limb exoskeleton robot on upper limb function in stroke patients. **Methods** A total of 40 stroke patients recruited in the Rehabilitation Treatment Center of the Shandong Provincial Third Hospital Affiliated to Shandong University from February 2022 to February 2023 were selected and randomly divided into control group and observation group, with 20 cases in each group. All patients were subjected to conventional rehabilitation treatment. In addition, upper limb exoskeleton robot rehabilitation training was performed in the control group, 25 min each time, once a day, 5 days a week, for 4 weeks. In the observation group, interactive scalp acupuncture combined with the upper limb exoskeleton robot was performed. The positioning standard for scalp acupuncture acupoints was the parieto-temporal anterior oblique line and parieto-parietal 2 lines, and the needle was left in place for 25 min, and twisting maneuver was applied once at an interval of 5 min, 1-2 min per time, once a day, 5 days a week, for 4 weeks in total. Pre- and post-treatment assessments of upper limb motor function before and after treatment were performed using the Fugl-meyer upper extremity motor function assessment scale (FMA-UE) within the domain of body functions and structures according to the International Classification of Functioning, Disability and Health Framework (ICF). In addition, within the ICF activity domain, the Wolf motor function test (WMFT) was utilized to assess patients' abilities to perform functional tasks with their upper limbs. Finally, within the ICF participation domain, the modified Barthel index (MBI) was used to evaluate the independence of patients in activities of daily living. **Results** (1) Body function and structure domain: Compared with those before treatment, the FMA-UE score of both groups significantly increased after 4 weeks of treatment ($P < 0.05$), and the observation group showed a more significant improvement in the FMA-UE score than the control group ($P < 0.05$). (2) Activity domain: Compared with those before treatment, the WMFT score of both groups significantly increased after 4 weeks of treatment ($P < 0.05$), and the observation group showed a more significant improvement in the WMFT score than the control group ($P < 0.05$). (3) Participation domain: The MBI score of both groups significantly increased after 4 weeks of treatment ($P < 0.05$), and the observation group showed a more significant improvement in the MBI score than the control group ($P < 0.05$). **Conclusion** Interactive scalp acupuncture combined with upper limb exoskeleton robot can significantly improve upper limb motor function, upper limb functional task performance, and activities of daily living in stroke patients.

KEY WORDS stroke; interactive scalp acupuncture; upper limb exoskeleton robot; closed-loop theory; upper limb function

DOI:10.3724/SP.J.1329.2024.01005